Heliyon 8 (2022) e12301

Contents lists available at ScienceDirect

Heliyon

journal homepage: www.cell.com/heliyon

Research article

Process schemes of ethanol coupling to C4 olefins based on a genetic algorithm for back propagation neural network optimization

Minghan Li [a,b], Lingling Zhao [b], Shuo Jin [a,b], Danlu Li [a,b], Jingyi Huang [b], Jiaxin Liu [c,d,*]

[a] School of Life and Pharmaceutical Sciences, Dalian University of Technology, 2 Dagong Road, Panjin, Liaoning 124221, PR China
[b] Panjin Campus, Dalian University of Technology, 2 Dagong Road, Panjin, Liaoning 124221, PR China
[c] China Nuclear Power Engineering Co., Ltd., 117 North West Third Ring Road, Beijing 100840, PR China
[d] School of Chemical Engineering, Dalian University of Technology, 2 Linggong Road, Dalian, Liaoning 116024, PR China

HIGHLIGHTS

- A scientific evaluation system for evaluating the production of C4 olefins.
- Construction of neural network and prediction of C4 olefin yield based on production indicators.
- Mixed Congruential method was improved and used to simulate experimental parameters.
- The yield of C4 olefin produced by ethanol under different experimental conditions was analyzed.

GRAPHICAL ABSTRACT

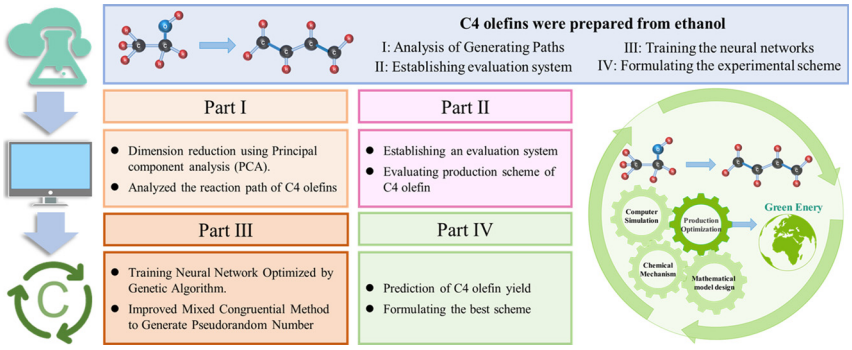

ARTICLE INFO

Keywords:
Ethanol to C4 olefins
TOPSIS
BPNN optimizes chemical process
Improved mixed congruential method

ABSTRACT

C4 olefin is an important feedstock for the chemical industry. Designing an effective and stable industrial process for preparing C4 olefin from renewable ethanol is crucial for further sustainable chemical production. In this study, a comprehensive evaluation system of an experimental scheme was constructed based on the Analytic Hierarchy Process/Entropy Weight Method-Technique for Order Preference by Similarity to Ideal Solution (AHP/EWM-TOPSIS) and Chemical production indicators. Using this evaluation system, a Back Propagation Neural Network (BPNN) based on a Genetic Algorithm (GA) was constructed after simulating C4 olefin production conditions using the Improved Mixed Congruential method. Subsequently, the production scheme with the highest evaluation score was determined when the temperature was not limited and when the temperature was lower than 350°C through a series of mathematical models. Overall, our mathematical models provide guidance for the commercial production of ethanol to butene and effectively reduce the risk of scaling up the chemical process to pilot or industrial scale.

1. Introduction

Low-carbon olefins are regarded as a significant raw material for the petrochemical industry and are widely used to manufacture packaging

* Corresponding author at: China Nuclear Power Engineering Co., Ltd., 117 North West Third Ring Road, Beijing 100840, PR China.
E-mail address: glu_jiaxinliu@mail.dlut.edu.cn (J. Liu).

https://doi.org/10.1016/j.heliyon.2022.e12301
Received 7 May 2022; Received in revised form 6 September 2022; Accepted 5 December 2022

materials, synthetic textiles, antifreeze, solvents, and coatings (Fu et al., 2022). However, traditional low-carbon olefin production technology based on fossil feedstocks has struggled to meet future demands of the low-carbon economy and stricter environmental protection requirements (Melisa et al., 2020). For example, the main 1,3-butadiene industrial production method involves the separation of this compound from petroleum steam cracking fractions (Gonzalez et al., 2019; Zhang et al., 2021). In turn, the increase in shale gas production containing large amounts of ethane has resulted in a decreased use of petroleum steam cracking to produce olefins, which will lead to the shortage of bulk chemicals such as C4 olefins (Le, 2018). Therefore, a process for preparing C4 olefins from unconventional and renewable resources must be developed given the burning of fossil feedstocks will adversely affect the world climate. Biomass is considered as a prime renewable resource for replacing fossil resources (Demirbas et al., 2009; Guo and Xiao, 2002). Based on the development of 'carbon neutralization', bioethanol produced from biomass has great prospects as a basic raw material of the chemical industry. Due to the sustainability and potential environmental benefits and economic value of bioethanol, the production of C4 olefins from bioethanol has aroused considerable research interest in the field of catalysis (Aditiya et al., 2016; Atsonios et al., 2015). In recent years, as researchers furthered the understanding of the catalyst activity center, the yield value of the C4 olefin reaction from ethanol has been significantly improved. (Dahan et al., 2021; Eagan et al., 2019; Katoh et al., 2008; Leon et al., 2011; Mayorov et al., 2021; Smith et al., 2016). Nevertheless, some problems remain and must be solved to realize the industrial application of ethanol for producing C4 olefins (Camacho et al., 2020; Jones, 2014). First, the selectivity of this reaction must be significantly enhanced. This improvement is a challenging task because the reaction mechanism for ethanol reacts to produce C4 olefins is complex and involves the production of many by-products. However, achieving high selectivity may effectively reduce the separation and purification cost of subsequent products. Therefore, how to improve the selectivity of the reaction is a problem worthy of attention. Another problem worth exploring is that the reaction mechanism of the production of C4 olefins from ethanol remains unclear. It is necessary to combine isotopic labeling method with in situ characterization techniques such as chemical probe identification or infrared characterization to try to explore the active site of chemical reaction catalysts (Wan et al., 2020; Ding et al., 2015).

Supported by experimental data, mathematical models can be used to predict the variation of the yield with other conditions in a multidimensional and dynamic manner, revealing the relationship between selectivity and catalyst types and operating parameters while providing some guidance for further experimental research and industrial production (Pedrozo et al., 2021). Therefore, performing simulation calculations before pilot and industrial tests is a viable strategy for effectively reducing trial and error costs.

An evaluation system consisting of the Analytic Hierarchy Process/Entropy Weight Method-Technique for Order Preference by Similarity to Ideal Solution (AHP/EWM-TOPSIS) was established to measure the quality of different C4 olefin production schemes. This evaluation system was based on five evaluation indexes: C4 olefin yield, temperature, ethanol conversion, catalyst mass (mg), and ethanol concentration (ml/min) (See Support Information for Experimental Data). The process conditions and the ethanol to C4 olefin reaction results are reported in the performance data table in the Support Information, totaling 114 experimental datasets. Based on these datasets, a Back Propagation Neural Network (BPNN) optimized using a Genetic Algorithm (GA), was constructed to predict the yield of C4 olefins under different Co loadings on SiO_2 and HAP catalyst systems, ethanol concentrations, and reaction temperatures. After using the AHP/EWM-TOPSIS evaluation system to select the most cost-effective experimental scheme, the experimental schemes were examined by reliability analysis. After deleting the experimental scheme with low reliability and replacing some experimental schemes, the C4 olefin production system with actual industrial production value was finally selected (Nobarzad et al., 2021).

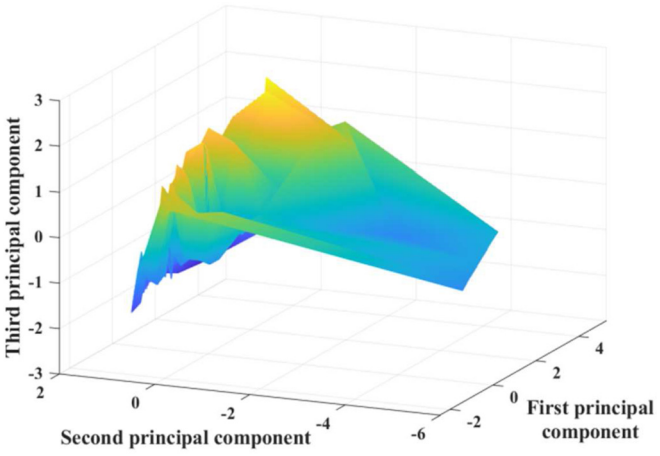

Fig. 1. Visualization of principal component 3D interpolation.

2. Preliminary analysis of C4 olefin production by ethanol coupling

2.1. PCA dimensionality reduction and visualization

Principal Component Analysis (PCA) is a Data Dimension Reduction Method based on Orthogonal Transformation. Which was used to reduce the dimension of seven groups of experimental parameters involved in the production of C4 olefins by ethanol coupling, including ethanol conversion, ethylene selectivity, and other indicators. For the specific use process of PCA in this article, please refer to the 3.1 section. Three principal components were obtained by dimension reduction as follows (Eq. (1), (2), (3)):

$$FP = 0.4522c_1 + 0.4221c_2 + 0.4623c_3 + 0.0858c_4 - 0.4581c_5 + 0.1039c_6 + 0.4190c_7 \quad (1)$$

$$SP = 0.1887c_1 - 0.2741c_2 + 0.2123c_3 - 0.7268c_4 + 0.3400c_5 + 0.3567c_6 + 0.2704c_7 \quad (2)$$

$$TP = -0.0600c_1 - 0.0064c_2 + 0.1962c_3 - 0.2592c_4 + 0.1153c_5 - 0.9041c_6 + 0.2450c_7 \quad (3)$$

In formulas (1), (2), and (3), c_1-c_7 are ethanol conversion, ethylene selectivity, C4 olefin selectivity, acetaldehyde selectivity, C4-C12 fatty alcohol selectivity with carbon number, methyl benzaldehyde/methyl benzyl alcohol selectivity, and selectivity to other products. FP, SP, and TP are the first, second, and third principal components, respectively, and the cumulative contribution rate was 87.97%. After three-dimensional interpolation, the visualization is as shown in Fig. 1.

As shown by preliminary analysis of the principal component interpolation (Fig. 1), when the second principal component value is close to 0, the value of the third principal component is high, and the third principal component is positively correlated with the first principal component; that is, when the second principal component is close to 0, the selectivity of methyl benzaldehyde and methyl benzyl alcohol is high. And at this time point, the ethanol conversion, ethylene selectivity, C4 olefin selectivity, and other indicators are positively correlated with the selectivity of methyl benzaldehyde and methyl benzyl alcohol. Subsequently, the generation path of C4 olefins was determined by correlation analysis of each index, and the evaluation system for the production of C4 olefins from ethanol was established by screening and weighting each index as well.

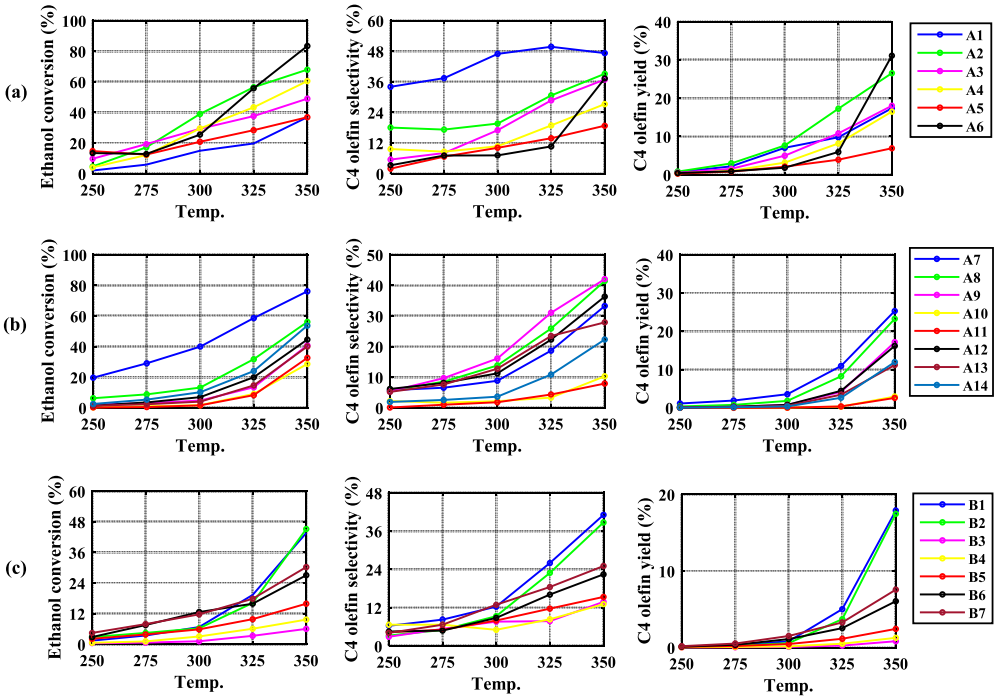

Fig. 2. The relationship of three indicators with temperature: (a) The change of ethanol conversion, C4 olefin selectivity, and C4 olefin yield with temperature when the catalyst dosage is more than 200 mg and the packing method is dilute phase packing; (b) When the catalyst dosage is less than or equal to 200 mg and the packing method is dilute phase packing, the ethanol conversion, C4 olefin selectivity and C4 olefin yield change with temperature; (c) It is the change of ethanol conversion, C4 olefin selectivity and C4 olefin yield with temperature when the catalyst dosage is less than or equal to 200 mg and the packing method is dense phase packing.

In addition to the data visualization after dimensionality reduction, the relationship between ethanol conversion, C4 olefin selectivity, and C4 olefin yield with time under different experimental schemes were also visualized in Fig. 2 (a)-(c).

The average Pearson Correlation Coefficients (PCC) between ethanol conversion, C4 olefin selectivity, and C4 olefin yield with the temperature of all experimental schemes are 0.93, 0.92, and 0.87, respectively, which are all greater than 0.8. Therefore, it can be considered that the ethanol conversion, C4 olefin selectivity, and C4 olefin yield of ethanol to olefin reaction are strongly and positively correlated with temperature. The average values of ethanol conversion, C4 olefin selectivity, and C4 olefin yield of the three sets of data at different temperatures were obtained as shown in Fig. 3 (a)-(c). It can be seen that for ethanol conversion and C4 olefin yield, Fig. 3 (a) > (b) > (c), that is, increasing the mass of catalyst can improve the ethanol conversion and C4 olefin yield (Fig. 3 (a) > (b)). Compared with dense phase packing, dilute phase packing can effectively improve the ethanol conversion and C4 olefin yield (Fig. 3 (a) > (b)); For C4 olefin selectivity, there is Fig. 3 (a) > (b) ≈ (c), that is, increasing the mass of catalyst can effectively improve the C4 olefin selectivity of ethanol to olefin reaction, but in the range of 250-350°C, the effect of packing method on C4 olefin selectivity is not obvious.

2.2. Path analysis of C4 olefin formation

The test results at different time points in the experiment of the production of C4 olefins from ethanol at 350°C were analyzed, changing the ethanol conversion, C4 olefin selectivity, C4-C12 fatty alcohol selectivity, ethylene selectivity, acetaldehyde selectivity, and methyl benzaldehyde/alcohol selectivity with time as shown in Fig. 4 (a), (b).

Throughout the reaction, acetaldehyde and ethylene selectivity gradually increased with time, showing a positive correlation (Fig. 4a). Conversely, the ethanol conversion and the selectivity of fatty alcohols with gradually decreased with time, although the latter increased to some extent from 200 to 240 min, and the selectivity of the two was negatively correlated with time overall. In addition, the selectivity of C4 olefins was not significantly correlated with the reaction time, whereas the selectivity of methyl benzaldehyde/methyl benzyl alcohol increased first and then decreased with the reaction time, albeit only slightly (Fig. 4b).

Further analysis of Fig. 4 shows that long-chain alcohols gradually cleaved into light alkenes, short-chain aldehydes, and so forth over the reaction time, thereby decreasing the selectivity. Once the reaction has been stabilized (150-273 min), C4 olefin selectivity was significantly and positively correlated with the selectivity of C4-C12 fatty alcohols, with Pearson Correlation Coefficients (PCC) of 0.84. Such a significant and positive correlation indicated that some fatty alcohols with C4-C12 carbons were decomposed to C4 olefins (Kyriienko et al., 2020). However, the selectivity of C4 olefins did not change significantly with time because alcohol/aldehyde dehydration is an endothermic reaction with a faster rate at higher temperatures (Ndou et al., 2003). The higher reaction temperature accelerated the cracking rate of C4-C12 fatty alcohols to C4 olefins (Phung and Busca, 2015). Therefore, although the selectivity of long-chain alcohols decreased with the reaction time, the selectivity of C4 olefins did not decrease significantly. This phenomenon also indicated the possible reason why the selectivity of the intermediate product (acetaldehyde) increased despite the decreased ethanol conversion because the equilibrium constant for ethanol dehydration to acetaldehyde becomes favorable at temperatures above 300 °C (Ramasamy and Wang, 2013).

Accordingly, the route of C4 olefin production from ethanol is shown in Fig. 5.

The possible pathway of methyl benzaldehydes/methyl benzyl alcohol production from ethanol is shown in Fig. 6 (Wang et al., 2019).

The possible pathway of cracking C4-C12 aliphatic alcohols into C4 olefins is shown in Fig. 7.

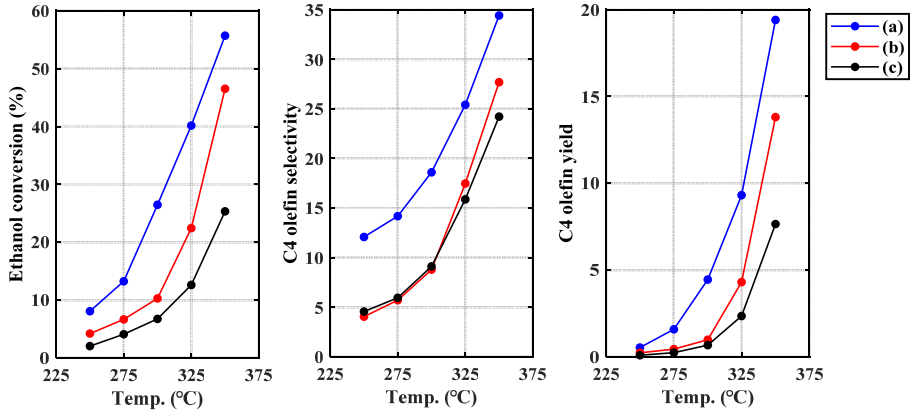

Fig. 3. Mean value graph of ethanol conversion, C4 olefin selectivity, and C4 olefin yield of three groups of data (a), (b), and (c) at a certain temperature. (a) Ethanol conversion average change over time. (b) C4 olefin selectivity average change over time. (c) C4 olefin yield average change over time.

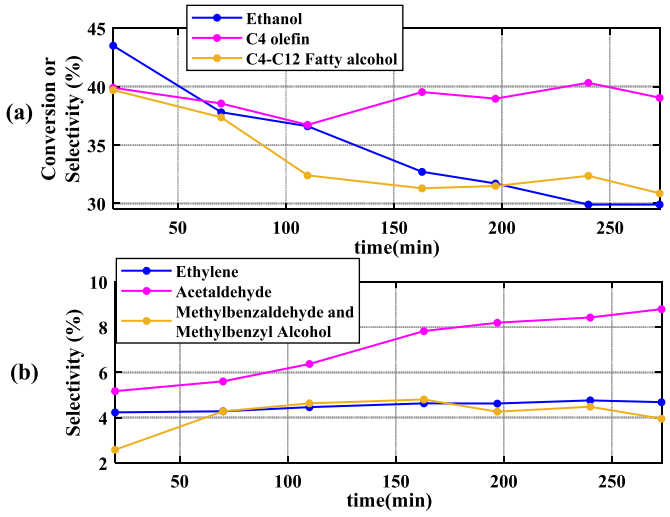

Fig. 4. Selectivity/conversion of each C4 olefin component prepared from ethanol as a function of time at 350°C (Reaction conditions can be found in Supporting Information). (a) The conversion of Ethanol, C4 olefin, and C4-C12 Fatty alcohol over time. (b) The conversion of ethylene, acetaldehyde, methyl benzaldehyde, and methyl benzyl alcohol over time.

3. Development of the mathematical model

3.1. Establishment of data dimension reduction model

For a production scheme to prepare C4 olefin from ethanol, seven outcome indicators are identified in this paper in addition to temperature: ethanol conversion, ethylene selectivity, C4 Olefin selectivity, acetaldehyde selectivity, C4-C12 Fatty alcohols, selectivity of methylbenzaldehyde and methyl benzyl Alcohol, selectivity of other products and C4 olefin yield. It is very difficult to directly visualize the seven groups of indicators in a figure, so Principal Component Analysis was used to reduce the dimension of the seven groups of indicators into three dimensions, and then the visualization can be carried out. In this paper, the dimensionality reduction process using Principal Component Analysis is as follows:

1) De-averaging

The first step of dimensionality reduction is de-averaging (i.e., decentralizing), which is subtracting the average value of each of the seven groups of indicator vectors.

2) Calculate the covariance matrix

Define matrix X, which is a 7×114 matrix. Each row of the matrix X represents an index after de-averaging, and each column represents a set of experimental data. Then, the covariance matrix $\frac{1}{n}XX^T$ should be calculated.

3) Calculate eigenvalues and eigenvectors

After obtaining the covariance matrix, the eigenvalues and eigenvectors of the covariance matrix $\frac{1}{n}XX^T$ can be obtained by the method of Eigendecomposition.

(4) Construct the eigenvector matrix P

Order the eigenvalues from the largest to the smallest, and select the largest k eigenvalues (k =3 in this paper). Then the corresponding k eigenvectors are taken as row vectors to form the eigenvector matrix P.

(5) Obtain the final dimensionality reduction result

After the eigenvector P is obtained, calculate the matrix $Y = PX$. Each row of matrix Y is a dimension after dimensionality reduction, and the element Y_{ij} in matrix Y represents the weight of indicator j on dimension i. The matrix Y as given in Eq. (4).

$$Y = \begin{bmatrix} 0.4522 & 0.4221 & 0.4623 & 0.0858 & -0.4581 & 0.1039 & 0.4190 \\ 0.1887 & -0.2741 & 0.2123 & -0.7268 & 0.3400 & 0.3567 & 0.2704 \\ -0.0600 & -0.0064 & 0.1962 & -0.2592 & 0.1153 & -0.9041 & 0.2450 \end{bmatrix} \quad (4)$$

Thus, the three groups of principal components after dimensionality reduction in Section 2.1 can be obtained.

3.2. Construction of the evaluation system

In addition to the yield of the target product, material costs and equipment loss should also be considered in chemical production (Guo et al., 2014; Fang et al., 2016; Wang et al., 2021). In this study, an evaluation system based on five indicators, namely C4 olefin yield, temperature, ethanol conversion, catalyst mass, and ethanol concentration was constructed. The Analytic Hierarchy Process (AHP) and the Entropy Weight Method (EWM) were used to weight the five indicators, subsequently applying the Technique for Order Preference by Similarity to Ideal Solution (TOPSIS) to calculate the scores of various catalyst combinations. In the final calculation results, the production system with the highest score had the highest comprehensive performance. The parameters involved in this section are outlined in Table 1.

3.2.1. AHP weighted C4 olefin yield

The yield of the target product C4 olefin is of great significance in the index system used to measure the total benefit of actual chemical production including five factors, C4 olefin yield, temperature, ethanol conversion, catalyst mass, and ethanol concentration. In this study, the Analytic Hierarchy Process was used to weight the yield of C4 olefins, constructing the judgment matrix as given in Eq. (5) (Note: The judgment matrix was only used to weight the yield of C4 olefins, and the other four indexes were weighted using the Entropy Weight Method).

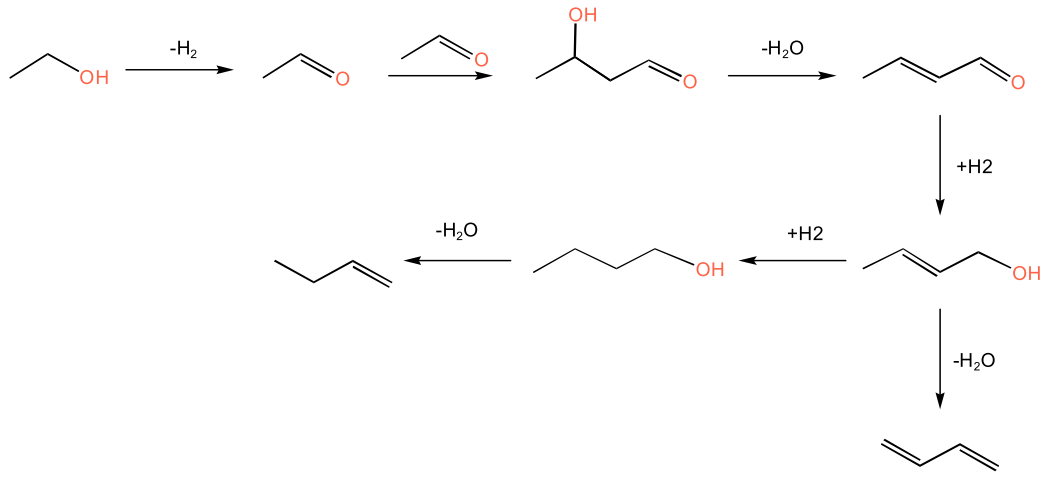

Fig. 5. Reaction mechanism of ethanol conversion into C4 olefins.

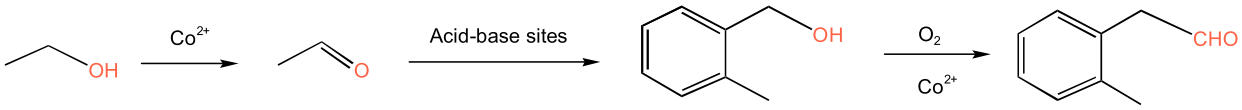

Fig. 6. The possible reaction mechanism of ethanol conversion into methyl benzaldehydes/methyl benzyl alcohols.

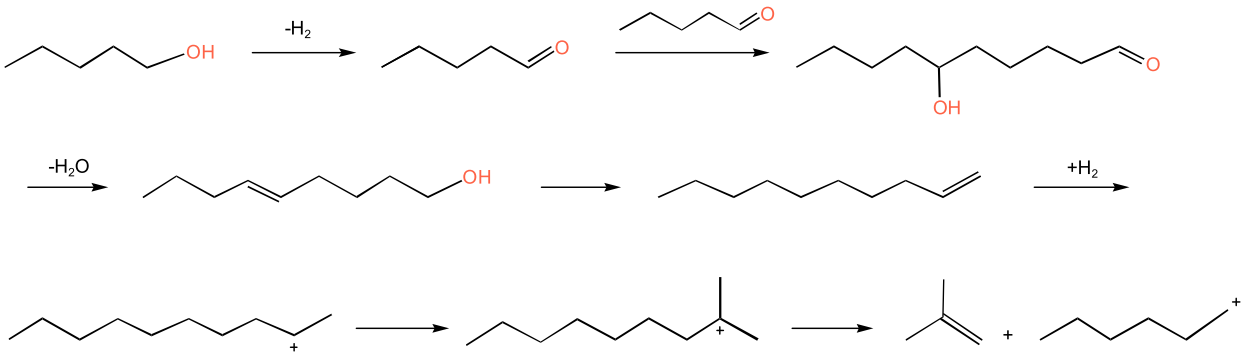

Fig. 7. The possible reaction mechanism of C4-C12 fatty alcohol cracking into C4 olefins.

$$A=\begin{bmatrix} 1 & 3 & 3 & 3 & 3 \\ 1/3 & 1 & 1 & 1 & 1 \\ 1/3 & 1 & 1 & 1 & 1 \\ 1/3 & 1 & 1 & 1 & 1 \\ 1/3 & 1 & 1 & 1 & 1 \end{bmatrix} \tag{5}$$

The judgment matrix $CR=0$ had a good consistency. Because A was a consistent matrix, an eigenvalue was 5, and the others were 0. The corresponding eigenvector was as shown in Eq. (6).

$$k[\frac{1}{A_{11}},\frac{1}{A_{12}},\frac{1}{A_{13}},\frac{1}{A_{14}},\frac{1}{A_{15}}]^T(k\neq 0) \tag{6}$$

The weight of C4 olefin yield in the index system was 0.429 because the value of A_{11} was 0.429.

3.2.2. Weighting other indexes using the entropy method

The Entropy Weight Method was used to weight the other three indexes except for C4 olefin yield with the following specific empowerment process:

1) Standardization of three indicators.

The standardization method used in this study was Min-Max standardization with the following standardization formula as given in Eq. (7).

$$Y_{ij}=\frac{X_{ij}-\min(X_i)}{\max(X_i)-\min(X_i)} \tag{7}$$

2) Calculation of the proportion of each data in the index. The proportion of each data in the index obtained through Eq. (8).

$$P_{ij}=\frac{Y_{ij}}{\sum_{i=1}^{n}Y_{ij}},\ i=1,\cdots,n,\ j=1,\cdots,m. \tag{8}$$

In this study, $n=114$, $m=4$.

3) Calculation of the information entropy of three indexes.

According to the definition of information entropy in information theory, the information entropy of a dataset can be obtained by Eq. (9).

$$E_j=-\ln(n)^{-1}\sum_{i=1}^{n}P_{ij}\ln P_{ij} \tag{9}$$

4) Calculation of the weight of each index by information entropy. In this paper, the weight of each index obtained by Eq. (10).

$$w_j=\frac{1-E_j}{k-\sum E_j},j=1,2,\cdots,m \tag{10}$$

k is the number of indicators, in this study, $k=4$.

Table 1. Symbols and definitions of the parameters.

parameter	explanation
A	Analytic Hierarchy Process Judgment Matrix
X_i	The i^{th} evaluation index vector except for C4 yield ($0 < i \leq 3$)
Y_i	Standardized index matrix
P_{ij}	the proportion of i^{th} data in the indicator j
E_j	Information entropy of indicator j
w_j	The weight of index j
x	A cost indicator that needs to be positivized
x'	The index x after positivizing
e_i	Ethanol conversion of the i^{th} catalytic combination after standardization ($0 < i \leq 114$)
e'_i	Ethanol conversion of the i^{th} catalytic combination after positivizing ($0 < i \leq 114$)
Z_{ij}	The j^{th} index value of the i^{th} catalytic combination after positivizing ($0 < i \leq 114$, $0 < j \leq 4$).
D_i^+	Distance between an experimental scheme and the optimal solution
D_i^-	Distance between an experimental scheme and the worst solution
$Score$	Final evaluation score of an experimental program
N	Number of neurons in hidden layer of BP neural network
K	Number of neurons in output layer of BP neural network
F	Individual fitness value of BP neural network
E	Standardized ethanol conversion vector
y_i	Prediction of catalyst combination i yield by BP neural network ($0 < i \leq 2970$)
O_i	The actual yield value of catalyst combination ($0 < i \leq 2970$)
a	Mixed multiplicative coefficient (constant)
b	Mixed identical addition coefficient (constant)
M	For the improved mixed congruential method, its period $\geq$ M

3.2.3. Scores calculated using the distance method

The Technique for Order Preference by Similarity to Ideal Solution was used to evaluate each test scheme. Among the five indicators of the evaluation system constructed in this study, improving the yield of C4 olefins is the purpose of production, and increasing ethanol conversion represents the efficient utilization of the reaction substrate and the increased production (Li et al., 2022). A low ethanol conversion affects the yield of C4 olefins, which cannot meet the production demand required product yield. As such, these two indicators are benefit indicators (A higher indicator value means a better production scheme). Since the energy can be saved and the service life of equipment can be extended at a lower reaction temperature (Iwamoto et al., 2011), the temperature of the reaction system is a cost indicator (A lower indicator value means a better production scheme). Similarly, ethanol concentration and catalyst mass are also cost indicators. In order to facilitate subsequent unified calculation, the following formula was used to convert cost (reaction system temperature, ethanol concentration, and catalyst mass) into benefit indicators (Eq. (11)):

$$x' = \max - x \tag{11}$$

After all indicators are unified into benefit indicators, the distance between all production schemes and optimal (or worst) production schemes are calculated as shown in Eq. (12).

$$D_i^+ = \sqrt{\sum_{j=1}^{4} W_j (Z_{ij} - 1)^2} \tag{12}$$

$$D_i^- = \sqrt{\sum_{j=1}^{4} W_j \times Z_{ij}^2} \tag{13}$$

The final *Score* of each production scheme can be obtained by Eq. (14).

$$Score = \frac{D_i^-}{D_i^+ + D_i^-} \tag{14}$$

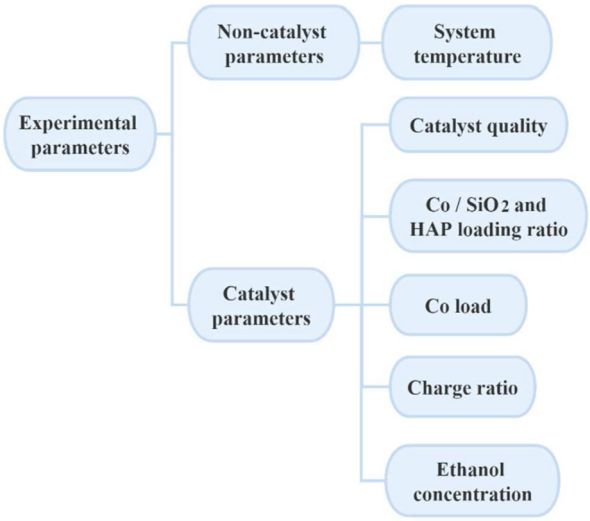

Fig. 8. Six parameters for designing the experimental scheme.

3.3. Construction of BP neural network based on genetic algorithm

In this part, a Back Propagation Neural Network based on a Genetic Algorithm (GA-BP) was constructed to predict the yield of C4 olefins under different experimental conditions. First, the values of six parameters shown in Fig. 8 were taken as input values and the yield of C4 olefins as the output value to construct the GA-BP. After that, in order to evaluate the merits and demerits of production schemes more comprehensively, the three indicators (catalyst mass, ethanol concentration, and temperature) were used to measure the cost of the chemical industry based on improving the yield of C4 olefin as much as possible. Finally, five production schemes with the best overall expectation score were selected as the recommended process conditions for chemical production.

3.3.1. Establishment of the back propagation neural network

The Back Propagation Neural Network (BPNN) is a multi-layer feed-forward neural network trained with the Back-Propagation Algorithm, which is currently the most widely used neural network. The principles of BPNN optimization using the genetic algorithm are that the initial weights and thresholds of the network are represented by the individuals and that the prediction error of BPNN initialized by each individual value is used as the fitness value of the individual. After selection, crossover, mutation, and other operations, the optimal individual is identified as the best initial weight of the BPNN. GABP has a stronger global optimization ability than the general BPNN, easily falling into the local optimum. The process of BPNN optimization using the genetic algorithm is shown in Fig. 9 (Genetic algorithm on the left and neural network on the right).

In this study, a three-layer neural network structure of $6 \times N \times 1$ was established, where 6 represents the number of neurons in the input layer, namely the six parameters that must be determined in the design experiment; N is the number of hidden layer neurons; 1 is the output term (yield of C4 olefins). In the three-layer network, the following approximate relationship was found between the number of neurons in the hidden layer N and the number of neurons in the input layer M (Eq. (15)) (Pourpasha et al., 2021; Abilov and Zeybek, 2000; Liu et al., 2001):

$$N = 2 \times M + 1 \tag{15}$$

The formula was combined with the Trial-and-Error method to determine the best N value of 13.

After determining the structure of the BPNN, this paper used a genetic algorithm to optimize the initial weights and thresholds of the BPNN in the following implementation steps:

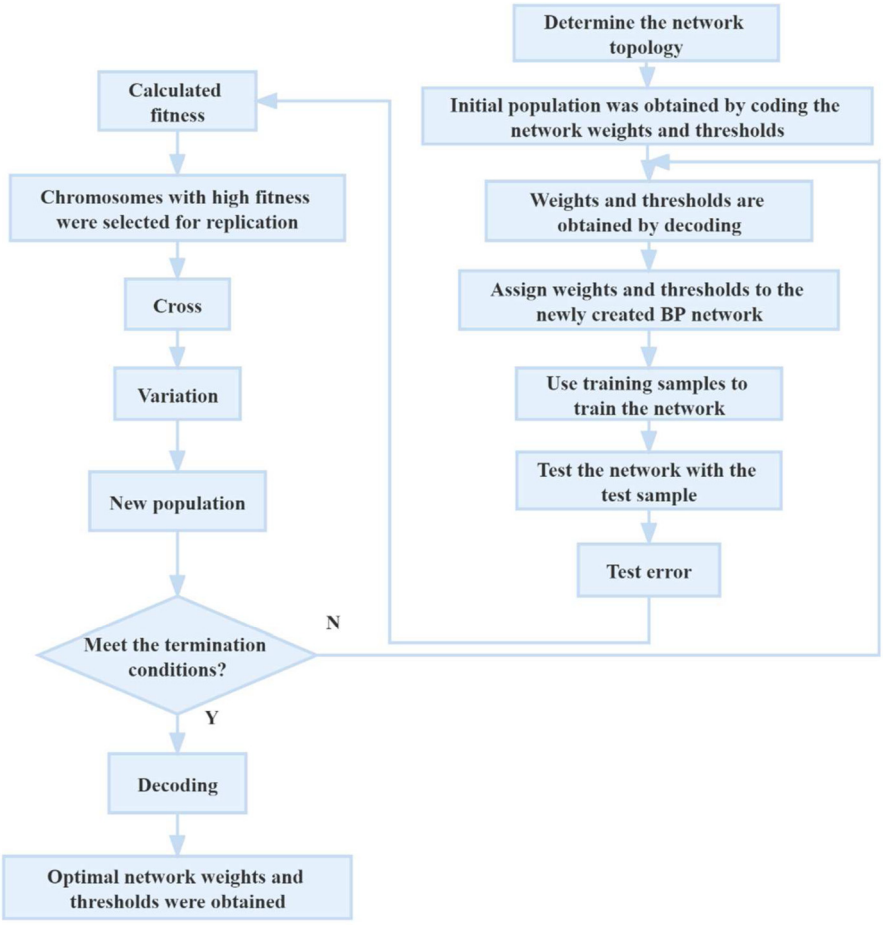

Fig. 9. Flow chart of the BP Neural Network algorithm optimized using Genetic Algorithm.

Step 1: Through the Real Coding of individuals in the initial population, the chromosome of each individual consists of four parts: the connection weight between the input layer and the hidden layer, the connection weight between the hidden layer and the output layer, the neuron threshold of the hidden layer, and the neuron threshold of the output layer.

Step 2: Based on the initial value of each individual chromosome, the initial weights and thresholds of the BPNN were calculated, and then the BPNN was trained using training data to predict the output of the system. The sum of the absolute value of the error between the predicted output and the expected output was used as the fitness value F of the individual. The calculation formula was given in Eq. (16).

$$F = k\sum_{i=1}^{n}\left|y_i - O_i\right| \tag{16}$$

Step 3: Individuals with the minimum fitness (error) were constructed by selection, crossover, and mutation of the genetic algorithm to set the initial weights and thresholds of the neural network. By this point, the number, weight, and threshold of neurons in the input layer, hidden layer, and output layer of the neural network had been clarified; then, the Levenberg-Marquardt algorithm was used as the learning algorithm of subsequent weights and thresholds for the BPNN. This algorithm combines the advantages of the Gauss-Newton algorithm with the Gradient Descent method and improves their shortages (the Gradient Descent method does not consider the accumulation of experience, and the convergence is slow; the initial value of the Gauss Newton algorithm may be too far from the local minimum), and the increment equation is as shown in Eq. (17).

$$(J^T W J + \lambda I)\delta x = -J^T W \Delta z \tag{17}$$

In the formula, $\Delta z = z - z\ (x)$, for the prediction error, W is the weight matrix; $j = dz/dx$, δx is the increment of the input values (or vector) x, and λ is the modification that reduces the cost function.

3.3.2. Improved mixed congruential method for generating a pseudorandom number

Before predicting the yield of C4 olefins, experimental parameters must be determined first. In this study, the computer algorithm was used to generate pseudo-random numbers, and then the pseudo-random numbers were combined into experimental schemes with different parameters. The mixed congruential method is a method commonly used to generate pseudo-random numbers, and its iterative formula as shown in Eq. (18), (19).

$$x_{i+1} = ax_i + bmod(M) \tag{18}$$

$$r_{i+1} = x_{i+1}M^{-1} \tag{19}$$

To lengthen the cycle period of the generated pseudo-random number and to overcome the drawback that any two pseudo-random numbers in a sequence generated using the mixed congruential method cannot be equal in a cycle, this paper improved the mixed congruential method after referring to previously reported data (Guo et al., 2014), with the following improved mixed homothetic method (Eq. (20), (21)):

$$x_{i+1} = ax_i + imod(M) \tag{20}$$

$$r_{i+1} = x_{i+1}M^{-1} \tag{21}$$

The improved mixed congruential method has a longer period, and multiple identical pseudo-random numbers can be generated in one cycle. In this study, $M = 2^{15} - 1$, $a = 2^7$, 2^8, 2^9, $M = 2^{16} - 1$, $a = 2^{11}$, $a = 2^{12}$,

Table 2. Weight table of five indexes.

Evaluation index name	Index weight	Weighting method
C4 olefin yield (%)	0.429	AHP
Temp. (°C)	0.155	EWM
Ethanol conversion (%)	0.212	EWM
Catalyst mass (mg)	0.143	EWM
Ethanol concentration (ml/min)	0.061	EWM

Table 3. Production scheme with high comprehensive scores.

	Number of catalyst combination	Temp. (°C)	Score (×10000)
Top 3 of all	A3	400	104.18
	A3	450	102.82
	A4	400	101.51
Top 3 of temp. <350°C	A2	325	92.59
	A3	325	89.62
	A4	325	88.68

$M = 2^{20}$, $a = 2^{10} + 1$ were selected as the initial parameters for generating six groups of pseudo-random numbers.

4. Results and discussion

4.1. Evaluation of different catalytic systems

The weights of temperature, ethanol conversion, catalyst mass, and ethanol concentration calculated using the Entropy Weight Method were multiplied by 0.571, and combined with the weight of C4 olefin yield calculated in the Analytic Hierarchy Process, five weights were obtained, as outlined in Table 2.

Taking the five weights into the calculation formula of the Technique for Order Preference by Similarity to Ideal Solution and the experimental schemes generated using the improved mixed congruential method, the score ranking was calculated as shown in Table 3.

In this part, the parameters of the optimal six groups of production schemes are shown in Table 4, and Table 5.

Considering the cost, equipment loss, and other factors, when the temperature limit was not required (the required temperature was lower than 350°C), the optimal catalyst combination was A3,400°C (A2,325°C). Simultaneously, the catalyst combination A3 still had an excellent performance at a low temperature (325°C). In actual chemical production, the catalyst combination A3 can be used to adjust the temperature of the reaction system between 325°C and 400°C (Guo et al., 2014; Meng et al., 2012; Chen et al., 2017). This scheme can reduce the energy consumption of the reactor and reasonably reduce the cost under the premise of a high C4 olefin yield.

4.2. Prediction of C4 olefin yield by GABP

4.2.1. GABP training results

A total of 2970 sets of sample data were obtained by cubic spline interpolation of 114 sets of experimental data (see supporting materials) and divided into two groups. The first 450 sets of each 500 datasets were selected as the training set, and the remaining 50 sets were selected as the test set (the last training set was 20 sets). The training dataset was loaded into the GA-BP neural network for training, and training was completed when the network training results met the preset accuracy requirements or the maximum number of iterations.

The performance of the neural network after training is shown in Fig. 10 (a), (b).

The weights and thresholds of neural network initialization using the genetic algorithm significantly accelerated the convergence speed of the BPNN. At the 226th training cycle, the mean square error of the neural network reached the minimum standard error (MSE = 1.2179×10^{-5}), and then the training was completed (Fig. 10(a)).

The test dataset was loaded into the GA-BP neural network to obtain the prediction output and the prediction error of the test set, as shown in Fig. 11.

In the prediction output and prediction error diagram shown in Fig. 11, the samples labeled with serial numbers of 0-250 were obtained by packing method I (dilute phase packing) and packing method II (dense phase packing) with a system temperature lower than 400°C. Moreover, the prediction error of the BPNN was within [−0.02, 0.02], indicating that the difference between the output value and the expected value was not large, which can meet the needs of the subsequent use of the neural network (KhazaiePoul et al., 2016; Li et al., 2017). The samples with serial numbers 251–270 were the prediction results of type II packing method with a system temperature of 400°C. The prediction error increased with the output value, which may be due to the lower number of training samples used in packing method II. In the subsequent prediction with the neural network, this paper used polynomial approximation to reduce the prediction error of the B-type packing method when the system temperature was 400°C (Zhang et al., 2013).

4.2.2. GABP simulation experiment results

In this part, six-dimensional pseudo-random numbers were generated using the improved mixed congruential method (Riera et al., 2021; Niederreiter and Shparlinski, 1999) to initialize the experimental parameters. Then, the BPNN that had been trained in 3.2.1 was used to predict the experimental results, simulate the real experimental conditions, and screen out the combinations of experimental parameters with a high expected yield of C4 olefins.

The pseudo-random number generated using the improved mixed congruential method was input into the trained BPNN, and generated the simulation results shown in Fig. 12.

When the temperature was equal to or greater than 400°C, the yield expectation of the charging method II was corrected in this study. The correction was based on the prediction error of sample Numbers 251-270 in part two. After regression analysis using the *cftool* tool in MATLAB, polynomial approximation was obtained by Eq. (22).

$$f(x) = 1.557x - 0.1923 \tag{22}$$

Correcting the yield expectation of packing method II by polynomial approximation led to the simulation results shown in Fig. 13.

Based on the simulation results before and after the correction, the combination of the five experimental parameters with the highest expected yield is presented in Table 6 (at a system temperature of 400°C).

To minimize the energy consumption of the reactor, the experimental parameters with the highest expected yield below 350°C were calculated as shown in Table 7 (catalyst mass ratio is 0.5).

The Technique for Order Preference by Similarity to Ideal Solution based on the Analytic Hierarchy Process and the Entropy Weight Method was used to comprehensively evaluate combinations of the above 10 experimental parameters (Tables 6 and 7). Among the five indicators, Co load and the packing method were not included in the calculation of the comprehensive evaluation. The catalyst mass was considered as an indicator of catalyst dosage (Liu et al., 2014). Therefore, among the four indexes involved in the Technique for Order Preference by Similarity to Ideal Solution, the catalyst mass, ethanol concentration, and system temperature were cost indicators, and the expected yield score was divided into benefit indicators.

The Analytic Hierarchy Process and the Entropy Weight Method were used to weigh the four indicators as shown in Table 8.

The comprehensive evaluation score of each catalyst combination was calculated according to the weight and sorted as shown in Table 9.

According to the comprehensive evaluation scores and expected yield scores, five experimental schemes were initially selected: numbers 550, 320, 440, 653, and 914. Scheme numbers 550 and 914 were included in the modest yield optimization group; and scheme numbers 320, 440, and 653 were included in the yield optimization group at low

Table 4. Specific information on the experimental scheme of highest comprehensive evaluation scores.

Number of catalyst combination	Temp. (°C)	Catalysts combination	Ethanol concentration (ml/min)	Score (×10000)
A3	400	200 mg 1wt%Co/SiO2- 200 mg HAP	0.9	104.18
A3	450	200 mg 1wt%Co/SiO2- 200 mg HAP	0.9	102.82
A4	400	200 mg 0.5wt%Co/SiO2- 200 mg HAP	1.68	101.51

Table 5. Specific information on the experimental scheme of highest comprehensive evaluation scores (Temp. <350°C).

Number of catalyst combination	Temp. (°C)	Catalysts combination	Ethanol concentration (ml/min)	Score (×10000)
A2	325	200 mg 2wt%Co/SiO2- 200 mg HAP	1.68	92.59
A3	325	200 mg 1wt%Co/SiO2- 200 mg HAP	0.9	89.62
A4	325	200 mg 0.5wt%Co/SiO2- 200 mg HAP	1.68	88.68

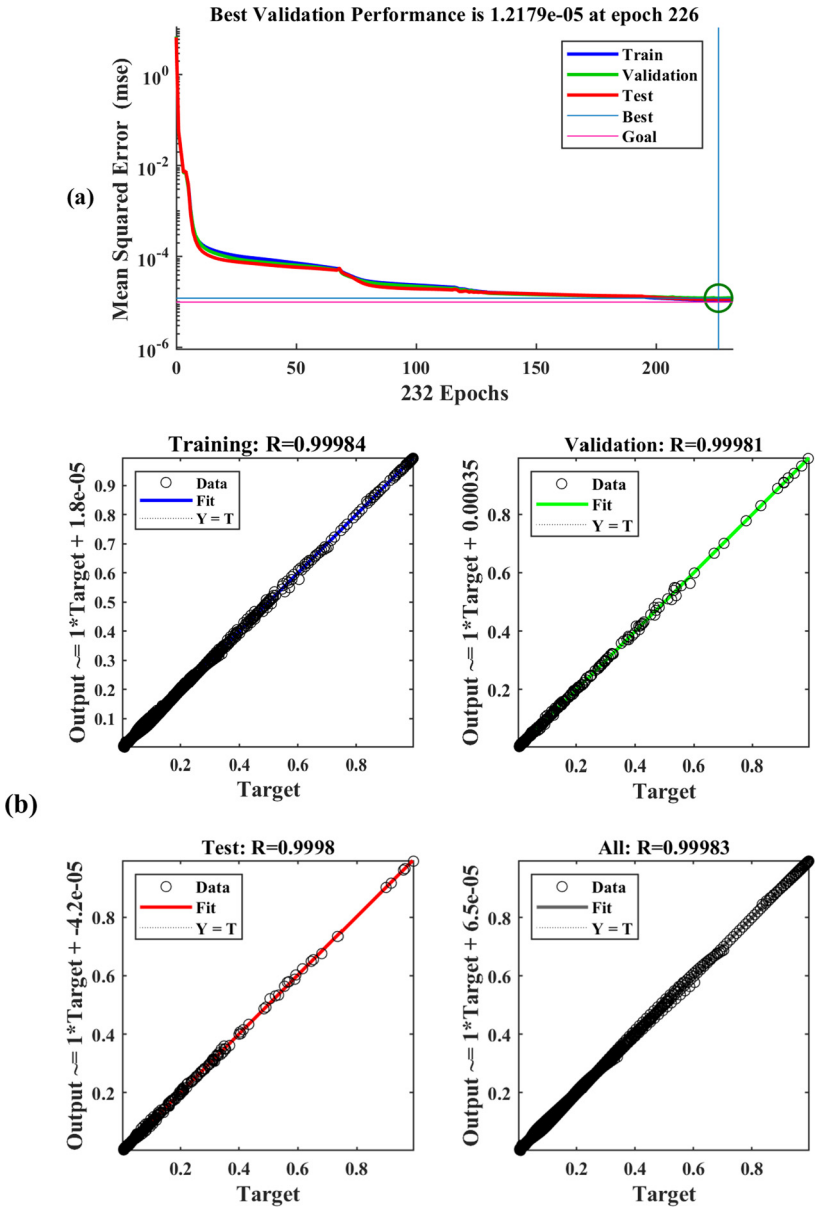

Fig. 10. Training results of neural networks: (a) Convergence, (b) Regression.

Table 6. Combination of the five experimental parameters with the highest expected yield.

No.	Catalyst mass (mg)	Mass ratio	Co load (wt%)	Ethanol concentration (ml/min)	Packing method
550	300	0.5	0.5	0.9	2
914	600	0.5	1	0.9	1
458	600	0.5	1	0.3	1
174	600	0.5	1	1.68	1
961	300	2	1	1.68	2

Table 7. Combination of the experimental parameters with the highest expected yield (<350°C).

No.	Catalyst mass (mg)	Co load (wt%)	Ethanol concentration (ml/min)	Packing method	Temp. (°C)
765	300	2	0.9	2	300
653	300	2	0.3	2	300
320	100	5	0.3	1	275
440	75	5	0.3	1	300
79	225	1	0.9	2	325

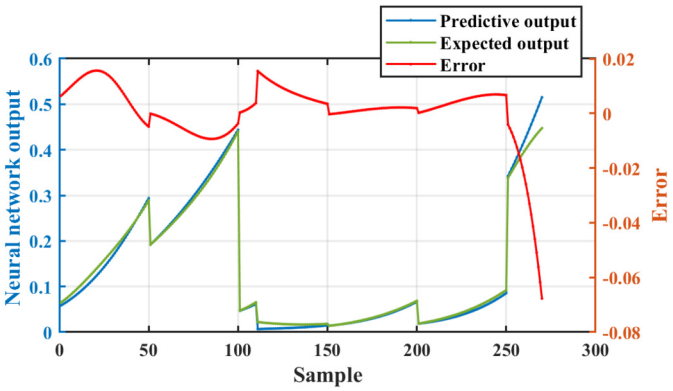

Fig. 11. Predictive output and error of test set.

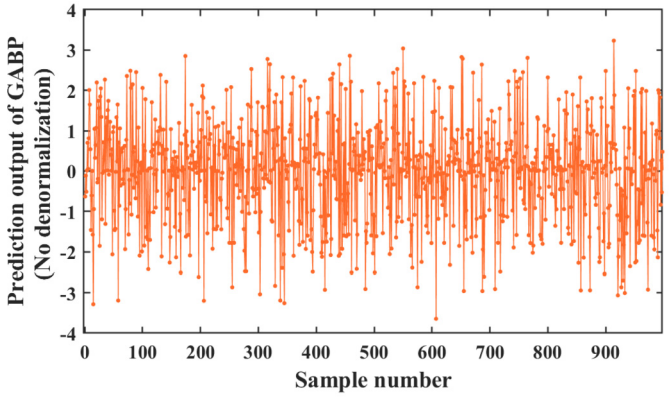

Fig. 12. BPNN simulation results.

Table 8. Weighting results of each index.

	Index name	Weighting method	
		EWM	AHP
Weight	Catalyst mass (%)	0.127	
	Ethanol concentration (ml/min)	0.249	
	Temp. (°C)	0.124	
	Prediction output (%)		0.5

temperatures. These five schemes were chosen as experimental designs for the following reasons:

No. 550: The comprehensive evaluation score and expected yield were the first.

No. 914: The comprehensive evaluation score was the fourth, the expected yield score was the second, and the three parameters differed greatly from number 550, which means that the mechanism for improving the expected yield of scheme number 550 may be different from that of the other schemes.

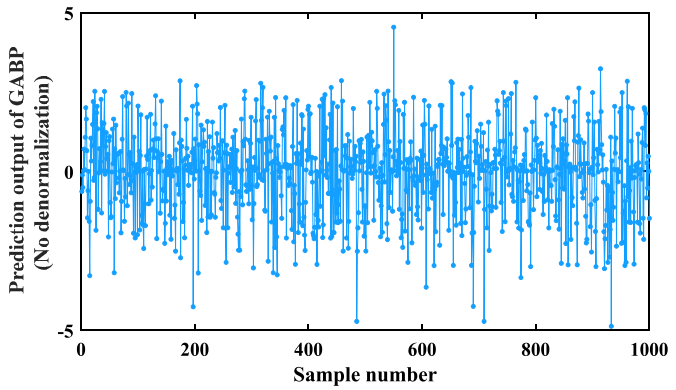

Fig. 13. Simulation results of the modified BPNN.

Table 9. Comprehensive evaluation and expected yield score.

Rank	No.	Comprehensive evaluation score	Expected yield score
1	550	100.00	100.00
2	320	59.90	8.32
3	440	57.43	8.11
4	653	54.95	14.99
5	914	47.03	36.59

No. 320: The comprehensive evaluation score was the second, and the expected yield score at a temperature lower than 350°C was the third.

No. 440: The comprehensive evaluation score was the third, and temperature lower than 350°C and the expected yield score were the second.

No. 653: The comprehensive evaluation score was the fourth, and the temperature lower than 350°C and the expected yield score were the second, with many parameters differing greatly from those of scheme numbers 320, 440, packing method II.

Subsequently, a feasibility analysis of the preliminary experimental program was conducted, and the final experimental program was determined.

Feasibility analysis and the final determination of the experimental plan:

A Co loading of 0.5 hinders a uniform dispersion on the catalyst surface, which is reduced (Elinson et al., 2019). However, a Co loading of 1 or 2 leads to Co aggregation on the catalyst surface, which is easily reduced at high temperatures. The best catalytic effect is achieved at these loadings (Al-Shafei et al., 2021). When the charging ratio is lower than 1, the increase in HAP content increases the number of alkaline

Table 10. Final experimental programs.

Rank	No.	Catalyst mass (mg)	Co load (wt%)	Ethanol concentration (ml/min)	Packing method	Temp. (°C)	Comprehensive evaluation score
1	320	200	5	0.3	1	275	59.90
2	440	75	2	0.3	2	300	57.43
3	653	300	2	0.3	2	300	54.95
4	914	600	0.5	1	1	400	47.03
5	961	300	2	1	2	400	27.83

sites in the catalyst (Pang et al., 2016; Carvalho et al., 2012; Cinelli et al., 2015), which promotes acetaldehyde conversion to the alkene. The optimum charging ratio is 1 because, when the loading ratio is greater than 1, the number of acid sites on the catalyst surface decreases with the HAP content, thereby decreasing the C4 olefin yield (Gao et al., 2013). The increase in ethanol concentration promotes ethanol conversion to acetaldehyde, which in turn promotes the production of C4 olefins (Song et al., 2020). Combined with the above analysis, under scheme number 550, the loading amount of Co was 0.5, the ethanol concentration was not high, and the loading ratio was lower than 1. By this time point, the HAP content was low, so a high yield was unreasonable under this condition. Therefore, scheme number 550 was deleted, and experimental program number 961 was added as the experimental program for optimizing the yield with charging method II.

In the optimal solution for a system temperature lower than 350°C, the Co loading value was greater than or equal to 1, requiring no correction.

The final five experimental programs for C4 olefin production from bioethanol with the best production cost performance expectations are outlined in Table 10 (catalyst mass ratio is 0.5).

5. Conclusions

This paper used mathematical modeling combined with experimental data to explore the practical industrial significance of different process conditions for the production of C4 olefins from bioethanol. By analyzing the effect of different catalyst formulations on the ethanol conversion and C4 olefin selectivity, a process with a higher C4 olefin yield was obtained. The results of this work can be summarized as follows (Ogihara et al., 2020; Akubo et al., 2019):

(1) An Analytic Hierarchy Process/Entropy Weight Method-Technique for Order Preference by Similarity to Ideal Solution method was constructed based on four factors: C4 olefin yield, temperature, ethanol conversion, and C4 olefin selectivity; then, 114 experimental datasets of C4 olefin production from ethanol were evaluated using this method, and six sets of process conditions with the highest cost performance under actual chemical production conditions were screened out.

(2) A GA-BP neural network was established, and the Analytic Hierarchy Process/Entropy Weight Method-Technique for Order Preference by Similarity to Ideal Solution evaluation system (AHP/EWM-TOPSIS) was combined with this neural network to select C4 olefin production conditions with the highest practical chemical production applicability. Using cubic spline interpolation for experimental data and training the neural network, the improved mixed congruential method was used to simulate various production parameters, and the GA-BP neural network was used to predict the C4 olefin yield.

Subsequently, the expected yield, catalyst dosage, ethanol concentration, and system temperature were selected as the evaluation indexes to construct the evaluation system of Analytic Hierarchy Process/Entropy Weight Method-Technique for Order Preference by Similarity to Ideal Solution, identifying five groups of ethanol production schemes for C4 olefins with high production cost performance.

In this paper, the chemical process conditions were optimized by mathematical modeling, which expanded the application of mathematical modeling and the process of preparing olefin from ethanol was improved. This approach may play a guiding role in the industrial production of C4 olefins from ethanol.

Declarations

Author contribution statement

Minghan Li: Conceived and designed the experiments; Performed the experiments; Wrote the paper.

Lingling Zhao; Jingyi Huang: Analyzed and interpreted the data.

Shuo Jin; Danlu Li: Performed the experiments.

Jiaxin Liu: Conceived and designed the experiments; Contributed reagents, materials, analysis tools or data; Wrote the paper.

Funding statement

This research did not receive any specific grant from funding agencies in the public, commercial, or not-for-profit sectors.

Data availability statement

Data included in article/supp. material/referenced in article.

Declaration of interest's statement

The authors declare no conflict of interest.

Additional information

Supplementary content related to this article has been published online at https://doi.org/10.1016/j.heliyon.2022.e12301.

Acknowledgements

The authors gratefully acknowledge the experimental data support from Dalian Institute of Chemical Physics, Chinese Academy of Sciences.

Appendix A. Supplementary material

Supplementary material related to this article can be found online at https://doi.org/10.1016/j.heliyon.2022.e12301.

References

Abilov, A., Zeybek, Z., 2000. Use of neural network for modeling of non-linear process integration technology in chemical engineering. Chem. Eng. Process. 39, 449–458.

Aditiya, H.B., Mahlia, T.M.I., Chong, W.T., Nur, H., Sebayang, A.H., 2016. Second generation bioethanol production: a critical review. Renew. Sustain. Energy Rev. 66, 631–653.

Akubo, K., Nahil, M.A., Williams, P.T., 2019. Pyrolysis-catalytic steam reforming of agricultural biomass wastes and biomass components for production of hydrogen/syngas. J. Energy Inst. 92, 1987–1996.

Al-Shafei, E.N., Albahar, M.Z., Aljishi, M.F., Aljishi, A.N., 2021. CO2 coupling reaction with methane by using trimetallic catalysts. J. Environ. Chem. Eng. 9, 106152.

Atsonios, K., Kougioumtzis, M.A., Panopoulos, K.D., Kakaras, E., 2015. Alternative thermochemical routes for aviation biofuels via alcohols synthesis: process modeling, techno-economic assessment and comparison. Appl. Energy 138, 346–366.

Camacho, C.E.C., Alonso-Fariñas, B., Perales, A.L.V., Vidal-Barrero, F., Ollero, P., 2020. Techno-economic and life-cycle assessment of one-step production of 1, 3-butadiene from bioethanol using reaction data under industrial operating conditions. ACS Sustain. Chem. Eng. 8, 10201–10211.

Carvalho, D.L., de Avillez, R.R., Rodrigues, M.T., Borges, L.E.P., Appel, L.G., 2012. Mg and Al mixed oxides and the synthesis of n-butanol from ethanol. Appl. Catal. A, Gen. 415, 96–100.

Chen, S.S., Maneerung, T., Tsang, D.C.W., Ok, Y.S., Wang, C.H., 2017. Valorization of biomass to hydroxymethylfurfural, levulinic acid, and fatty acid methyl ester by heterogeneous catalysts. Chem. Eng. J. 328, 246–273.

Cinelli, B.A., Castilho, L.R., Freire, D.M.G., Castro, A.M., 2015. A brief review on the emerging technology of ethanol production by cold hydrolysis of raw starch. Fuel 150, 721–729.

Dahan, H.O., Landau, M.V., Herskowitz, M., 2021. Effect of surface acidity-basicity balance in modified ZnxZryOz catalyst on its performance in the conversion of hydrous ethanol to hydrocarbons. Ind. Eng. Chem. Res. 95, 156–169.

Demirbas, M.F., Balat, M., Balat, H., 2009. Potential contribution of biomass to the sustainable energy development. Energy Convers. Manag. 50, 1746–1760.

Ding, K., Gulec, A., Johnson, A.M., Schweitzer, N.M., Stucky, G.D., Marks, L.D., Stair, P.C., 2015. Identification of active sites in CO oxidation and water-gas shift over supported Pt catalysts. Science 350, 189–192.

Eagan, N.M., Moore, B.M., McClelland, D.J., Wittrig, A.M., Canales, E., Lanci, M.P., Huber, G.W., 2019. Catalytic synthesis of distillate-range ethers and olefins from ethanol through Guerbet coupling and etherification. Green Chem. 21, 3300–3318.

Elinson, M.N., Vereshchagin, A.N., Anisina, Y.E., Krymov, S.K., Fakhrutdinov, A.N., Egorov, M.P., 2019. Selective multicomponent'one-pot' approach to the new 5-(4-hydroxy-6-methyl-2-oxo-2H-pyran-3-yl)chromeno 2, 3-b pyridine scaffold in pyridine-ethanol catalyst/solvent system. Monatsh. Chem. 150, 1073–1078.

Fang, Z., Qiu, T., Chen, B.Z., 2016. Improvement of ethylene cracking reaction network with network flow analysis algorithm. Comput. Chem. Eng. 91, 182–194.

Fu, X.X., Li, J.P., Li, Z.Q., Liu, Y., Feng, C.X., Wang, H.Y., Zhao, Z.P., Liu, Q.Y., 2022. Selective conversion of 2-methylfuran to 3-acetyl-1-propanol in water over Pd@HZSM-5 catalyst with balanced metal-acid cooperation. J. Catal. 413, 648–657.

Gao, D., Feng, Y., Yin, H., Wang, A., Jiang, T., 2013. Coupling reaction between ethanol dehydrogenation and maleic anhydride hydrogenation catalyzed by Cu/Al_2O_3, Cu/ZrO_2, and Cu/ZnO catalysts. Chem. Eng. J. 233, 349–359.

Gonzalez, G.M.C., Murciano, R., Perales, A.L.V., Martinez, A., Vidal-Barrero, F., Campoy, M., 2019. Ethanol conversion into 1, 3-butadiene over a mixed Hf-Zn catalyst: a study of the reaction pathway and catalyst deactivation. Appl. Catal. A, Gen. 570, 96–106.

Guo, S.B., Xiao, X.C., 2002. Interval prediction of pseudo-random sequences generated by multiplicative congruential method. Chin. J. Radio Sci. 17, 250–253.

Guo, X.C., Wang, X.C., Guan, J., Chen, X.F., Qin, Z.F., Mu, X.D., Xian, M., 2014. Selective hydrogenation of D-glucose to D-sorbitol over Ru/ZSM-5 catalysts. Chin. J. Catal. 35, 733–740.

Iwamoto, M., Kasai, K., Haishi, T., 2011. Conversion of ethanol into polyolefin building blocks: reaction pathways on nickel ion-loaded mesoporous silica. ChemSusChem 4, 1055–1058.

Jones, M.D., 2014. Catalytic transformation of ethanol into 1, 3-butadiene. Cent. Eur. J. Chem. 8, 53.

Katoh, M., Yamazaki, T., Kikuchi, N., Okada, Y., Yoshikawa, T., Wada, M., 2008. Conversion of bio-ethanol into hydrocarbons over HZSM-5 catalyst. Kagaku Kogaku Ronbunshu 34, 396–401.

KhazaiePoul, A., Soleimani, M., Salahi, S., 2016. Solubility prediction of disperse dyes in supercritical carbon dioxide and ethanol as co-solvent using neural network. Chin. J. Chem. Eng. 24, 491–498.

Kyriienko, P.I., Larina, O.V., Soloviev, S.O., Orlyk, S.M., 2020. Catalytic conversion of ethanol into 1, 3-butadiene: achievements and prospects: a review. Theor. Exp. Chem. 56, 213–242.

Le, M.T., 2018. An assessment of the potential for the development of the shale gas industry in countries outside of North America. Heliyon 4, e00516.

Leon, M., Diaz, E., Ordonez, S., 2011. Ethanol catalytic condensation over Mg-Al mixed oxides derived from hydrotalcites. Catal. Today 164, 436–442.

Li, H., Zhang, Z.E., Liu, Z.J., 2017. Application of artificial neural networks for catalysis: a review. Catalysts 7, 306.

Li, Z.L., Gao, M.X., Wang, S., Zhang, X., Gao, P.Y., Yang, Y.X., Sun, W.P., Liu, Y.F., Pan, H.G., 2022. In-situ introduction of highly active TiO for enhancing hydrogen storage performance of LiBH4. Chem. Eng. J. 433, 134485.

Liu, Y., Liu, Y., Liu, D.Z., Cao, T., Han, S., Xu, G.H., 2001. Design of CO2 hydrogenation catalyst by an artificial neural network. Comput. Chem. Eng. 25, 11–12.

Liu, Q., Dong, X., Liu, Z., 2014. Performance of $Ni/Nano\text{-}ZrO_2$ catalysts for CO preferential methanation. Chin. J. Chem. Eng. 22, 131–135.

Mayorov, P., Asabina, E., Zhukova, A., Osaulenko, D., Pet'kov, V., Lavrenov, D., Kovalskii, A., Fionov, A., 2021. Catalytic properties of the framework-structured zirconium-containing phosphates in ethanol conversion. Res. Chem. Intermed. 47, 3645–3659.

Melisa, O., Mauricio, M., Andrea, D.L., Elisa, V., Alejandro, A., Nestor, T., Juan, B., 2020. Catalytic assessment of solid materials for the pyrolytic conversion of low-density polyethylene into fuels. Heliyon 6, e05080.

Meng, T., Mao, D.S., Guo, Q.S., Lu, G.Z., 2012. The effect of crystal sizes of HZSM-5 zeolites in ethanol conversion to propylene. Catal. Commun. 21, 52–57.

Ndou, A.S., Plint, N., Coville, N.J., 2003. Dimerisation of ethanol to butanol over solid-base catalysts. Appl. Catal. A, Gen. 251, 337–345.

Niederreiter, H., Shparlinski, I.E., 1999. On the distribution and lattice structure of nonlinear congruential pseudorandom numbers. Finite Fields Appl. 5, 246–253.

Nobarzad, M.J., Tahmasebpoor, M., Imani, M., Pevida, C., Heris, S.Z., 2021. Improved CO2 adsorption capacity and fluidization behavior of silica-coated amine-functionalized multi-walled carbon nanotubes. Chem. Eng. J. 9, 105786.

Ogihara, H., Imai, N., Kurokawa, H., 2020. Decomposition and coupling of methane over $Pd–Au/Al_2O_3$ catalysts to form COx-free hydrogen and C2 hydrocarbons. Int. J. Hydrog. Energy 45, 33612–33622.

Pang, J.F., Zheng, M.Y., He, L., Li, L., Pan, X.L., Wang, A.Q., Wang, X.D., Zhang, T., 2016. Upgrading ethanol to n-butanol over highly dispersed Ni-MgAlO catalysts. J. Catal. 344, 184–193.

Pedrozo, H.A., Rodriguez Reartes, S.B., Vecchietti, A.R., Diaz, M.S., Grossmann, I.E., 2021. Optimal design of ethylene and propylene coproduction plants with generalized disjunctive programming and state equipment network models. Comput. Chem. Eng. 149, 107298.

Phung, T.K., Busca, G., 2015. Diethyl ether cracking and ethanol dehydration: acid catalysis and reaction paths. Chem. Eng. J. 272, 92–101.

Pourpasha, H., Farshad, P., Heris, S.Z., 2021. Modeling and optimization the effective parameters of nanofluid heat transfer performance using artificial neural network and genetic algorithm method. Energy Rep. 7, 8447–8464.

Ramasamy, K.K., Wang, Y., 2013. Catalyst activity comparison of alcohols over zeolites. J. Energy Chem. 22, 65–71.

Riera, C., Roy, T., Sarkar, S., Stanica, P., 2021. A hybrid inversive congruential pseudo-random number generator with high period. Eur. J. Appl. Math. 14, 1–18.

Smith, C., Dagle, V.L., Flake, M., Ramasamy, K.K., Kovarik, L., Bowden, M., Onfroy, T., Dagle, R.A., 2016. Conversion of syngas-derived C-2+ mixed oxygenates to C-3-C-5 olefins over ZnxZryOz mixed oxide catalysts. Catal. Sci. Technol. 6, 2325–2336.

Song, X.J., Wang, J., Yang, L.B., Pan, H.Y., Zheng, B., 2020. The transformation strategies between homogeneous and heterogeneous catalysts for the coupling reactions of CO_2 and epoxides/olefins. Inorg. Chem. Commun. 121, 108197.

Wan, G., Zhang, G., Lin, X.M., 2020. Toward efficient carbon and water cycles: emerging opportunities with single-site catalysts made of 3d transition metals. Adv. Mater. 32, 1905548.

Wang, Q.N., Weng, X.F., Zhou, B.C., Lv, S.P., Miao, S., Zhang, D.L., Han, Y., Scott, S.L., Schüth, F., Lu, A.H., 2019. Direct, selective production of aromatic alcohols from ethanol using a tailored bifunctional cobalt-hydroxyapatite catalyst. ACS Catal. 9, 7204–7216.

Wang, Q., Liu, C.Y., Luo, R., Li, X.D., Li, D.T., Macian-Juan, R., 2021. Thermo-economic analysis and optimization of the very high temperature gas-cooled reactor-based nuclear hydrogen production system using copper-chlorine cycle. Int. J. Hydrog. Energy 46, 31563–31585.

Zhang, X.L., Liu, Z.W., Xu, X.L., Yue, H.J., Tian, G., Feng, S.H., 2013. Hydrothermal synthesis of 1-butanol from ethanol catalyzed with commercial cobalt powder. ACS Sustain. Chem. Eng. 1, 1493–1497.

Zhang, J.Y., Yoo, E.J., Davison, B.H., Liu, D.X., Schaidle, J.A., Tao, L., Li, Z.L., 2021. Towards cost-competitive middle distillate fuels from ethanol within a market-flexible biorefinery concept. Green Chem. 23, 9534–9548.